

CONFIDENTIAL

Copy 7
RM L53122

NACA RM L53122

NACA

RESEARCH MEMORANDUM

STATIC LONGITUDINAL STABILITY AND CONTROL CHARACTERISTICS
OF A 1/16-SCALE MODEL OF THE DOUGLAS D-558-II RESEARCH
AIRPLANE AT MACH NUMBERS OF 1.61 AND 2.01

By M. Leroy Spearman

Langley Aeronautical Laboratory
Langley Field, Va.

UNCLASSIFIED

To _____

By authority of *NACA Res also effective*
2 RN-128 Date *June 24, 1958*

AMT 8-13-58

CLASSIFIED DOCUMENT

This material contains information affecting the National Defense of the United States within the meaning of the espionage laws, Title 18, U.S.C., Secs. 793 and 794, the transmission or revelation of which in any manner to an unauthorized person is prohibited by law.

NATIONAL ADVISORY COMMITTEE
FOR AERONAUTICS

WASHINGTON
November 6, 1953

LANGLEY AERONAUTICAL LABORATORY
LANGLEY FIELD, VIRGINIA

CONFIDENTIAL



NATIONAL ADVISORY COMMITTEE FOR AERONAUTICS

RESEARCH MEMORANDUM

STATIC LONGITUDINAL STABILITY AND CONTROL CHARACTERISTICS
OF A 1/16-SCALE MODEL OF THE DOUGLAS D-558-II RESEARCH
AIRPLANE AT MACH NUMBERS OF 1.61 AND 2.01

By M. Leroy Spearman

SUMMARY


An investigation has been conducted in the Langley 4- by 4-foot supersonic pressure tunnel at Mach numbers of 1.61 and 2.01 to determine the static longitudinal stability and control characteristics of a 1/16-scale model of the Douglas D-558-II research airplane.

The results of the investigation indicated a high degree of longitudinal stability that decreased slightly with increasing Mach number and lift coefficient. The trim lift coefficient obtained with the maximum horizontal-tail deflection of -6° was 0.557 at a Mach number of 1.61 and 0.425 at a Mach number of 2.01. The maximum trimmed lift-to-drag ratio was about 3.2 at a Mach number of 1.61 and about 3 at a Mach number of 2.01.

For a constant wing loading the control position required to trim with increasing Mach number (stick-position stability) was found to change from an unstable to a stable variation with increasing altitude.

INTRODUCTION

Various investigations have been concerned with the aerodynamic characteristics of the Douglas D-558-II research airplane and the airplane is currently undergoing flight tests by the National Advisory Committee for Aeronautics at Edwards Air Force Base. An investigation of a 1/16-scale model of the airplane has been conducted in the Langley 4- by 4-foot supersonic tunnel to supplement the flight-test results and to extend the results of other tunnel investigations to higher supersonic Mach numbers. The results of the lateral-stability investigation at Mach numbers of 1.61 and 2.01 are presented in reference 1. This paper presents



the longitudinal stability and control characteristics for Mach numbers of 1.61 and 2.01 and includes a correlation with results presented in reference 2 at high subsonic speeds and at a Mach number of 1.2.

COEFFICIENTS AND SYMBOLS

The results of the investigation are presented as standard NACA coefficients of forces and moments. The data are referred to the stability axis system (fig. 1) with the reference center of gravity at 25 percent of the wing mean aerodynamic chord. The coefficients and symbols are defined as follows:

C_L	lift coefficient, $-Z/qS$
C_D	drag coefficient, $-X/qS$
C_m	pitching-moment coefficient, $M'/qS\bar{c}$
Z	force along Z-axis
X	force along X-axis
M'	moment about Y-axis
q	free-stream dynamic pressure
S	total wing area including body intercept
\bar{c}	wing mean aerodynamic chord
M	Mach number
i_t	stabilizer incidence angle with respect to body center line, deg
α	angle of attack, deg
δ_e	elevator deflection with respect to stabilizer chord, deg
L/D	lift-drag ratio, C_L/C_D
ΔC_D	increment of drag above minimum drag
$\Delta C_D/C_L^2$	drag-due-to-lift factor
ϵ	effective downwash angle at tail, deg

x_{np}	neutral-point location, percent \bar{c}
x_{no}	tail-off aerodynamic-center location, percent \bar{c}
W	weight
h	altitude
Δi_t	increment of stabilizer deflection, deg
Δa_n	increment of normal acceleration, g-units
C_{L_α}	lift-curve slope, $\frac{dC_L}{d\alpha}$
$\frac{dC_m}{di_t}$	rate of change of pitching-moment coefficient with stabilizer deflection for constant angle of attack
$\frac{dC_m}{d\delta_e}$	rate of change of pitching-moment coefficient with elevator deflection for constant angle of attack and stabilizer incidence
$\frac{d\epsilon}{dC_L}$	rate of change of effective downwash angle with lift coefficient
$\frac{d\epsilon}{d\alpha}$	rate of change of effective downwash with angle of attack

MODEL AND APPARATUS

A three-view drawing of the model is presented in figure 2. Details of the wing fences are presented in figure 3. The vertical tail of the model is the same as that originally used on the airplane. However, a slightly extended tail is now in use on the airplane. In addition, the afterportion of the fuselage of the model was enlarged to accommodate the balance. The geometric characteristics of the model are presented in table I. Coordinates for the body are given in table II and for the wing fences in table III.

The model was equipped with a wing having 35° of sweep of the 0.30-chord line, aspect ratio 3.57, taper ratio 0.565, and NACA 63-010 airfoil sections normal to the 0.30-chord line. The wing had 3° of incidence with respect to the fuselage center line and 3° of negative dihedral.

The model wing section differs from that of the airplane in that the wing tip section of the airplane is an NACA 63₁-012 section.

Deflections of the stabilizer and elevator were set manually. The wing, vertical tail, and stabilizer were removable to facilitate the investigation of various combinations of component parts.

Force and moment measurements were made through the use of a six-component internal strain-gage balance.

TEST CONDITIONS

The conditions for the tests were:

Mach number1.61	2.01
Reynolds number, based on wing \bar{c}	$.1.90 \times 10^6$	1.52×10^6
Stagnation dewpoint, $^{\circ}\text{F}$	-20	-25
Stagnation pressure, lb/sq in.	15	14
Stagnation temperature, $^{\circ}\text{F}$	110	110
Mach number variation	± 0.01	± 0.015
Flow angle in horizontal or vertical plane, deg	± 0.1	± 0.1

CORRECTIONS AND ACCURACY

The angle of attack was corrected for the deflection of the balance and sting under load. No corrections were applied to the data to account for the tunnel flow variations. The base pressure was measured and the drag force was corrected to a base pressure equal to the free-stream static pressure.

The estimated errors in the individual measured quantities are as follows:

C_L	± 0.003
C_D	± 0.001
C_m	± 0.0006
α , deg	± 0.1
i_t , deg	± 0.1
δ_e , deg	± 0.1

RESULTS

Aerodynamic characteristics for the body alone (based on wing area and mean aerodynamic chord) were obtained for a Mach number of 1.61 only (fig. 4) but no appreciable change would be expected in these characteristics at a Mach number of 2.01.

The aerodynamic characteristics in pitch of the body—vertical-tail configuration and the body—vertical-tail—horizontal-tail configuration with several values of horizontal-tail incidence angle are presented in figure 5 for Mach numbers of 1.61 and 2.01.

Variations of C_m , C_D , and α with C_L for the complete model with various horizontal-tail incidence angles and with the horizontal tail removed are presented in figure 6 for both Mach numbers. The effect of elevator deflection on the aerodynamic characteristics in pitch at both Mach numbers for $i_t = 0^\circ$ is shown in figure 7. The maximum trim lift coefficient obtained with the maximum horizontal-tail deflection of -6.0° is 0.557 at $M = 1.61$ and 0.425 at $M = 2.01$ (see fig. 6). The increment in trim lift coefficient provided by the maximum elevator deflection for the model (-13.1°) at $i_t = 0^\circ$ is 0.13 at $M = 1.61$ and 0.094 at $M = 2.01$ (see fig. 7). It should be pointed out that the maximum elevator deflection for the full-scale airplane is about -25° .

The nonlinear variation of C_m with C_L for the complete model in the higher C_L range, which is apparently caused by shifts in the wing-body aerodynamic-center location, may result in a nonlinear change in the angle of attack (pitch-up or pitch-down) for abrupt control deflection maneuvers (see fig. 6(a), $i_t = -6^\circ$).

The variation of control deflection, lift-drag ratio, C_D , and α with C_L for trimmed flight ($C_m = 0$) for both Mach numbers is presented in figure 8(a) for horizontal-tail control and in figure 8(b) for elevator control at $i_t = 0^\circ$. The maximum trim L/D at $M = 1.61$ was about 3.2 and at $M = 2.01$ was about 3.0.

The drag variation due to lift for trimmed flight (fig. 9) is in reasonably good agreement with that which would be expected from consideration of the reciprocal of the lift-curve slope. The following values are obtained:

M	$\Delta C_D / C_L^2$	$1/57.3 C_{L_\alpha}$
1.61	0.36	0.35
2.01	.46	.42

The variation of C_m with i_t for various angles of attack is shown in figure 10. Limited data available for the model without the wing indicate little effect of the wing on the slope dC_m/di_t at $\alpha = 0^\circ$ (fig. 11).

The variation of the effective downwash angle ϵ with C_L for the complete model and of ϵ with α for the model with and without the wing is presented in figure 12 for both Mach numbers. These results were obtained from figures 5, 6, and 10 using the relation $\epsilon = \alpha + i_t - \alpha_t$ where α_t (horizontal-tail angle of attack) is assumed to be zero for those angles of attack at which a tail-on C_m curve intersects the tail-off C_m curve. At other angles of attack the relation $\alpha_t = \frac{\Delta C_m}{dC_m/di_t}$ was used where ΔC_m is the increment between a tail-on and tail-off pitching-moment curve. Throughout the angle-of-attack range a large portion of the downwash appears to be induced by the flow over the body and above $\alpha = 5^\circ$ an increase in the wing downwash results in an increase in $d\epsilon/d\alpha$.

The variation of the neutral-point location with C_L (fig. 13) indicates a large static margin (about 37 percent of the mean aerodynamic chord) that tends to decrease with Mach number and with increasing C_L .

The computed variation of the lift coefficient required for level flight with wing loading for various altitudes is shown in figure 14 for both Mach numbers. Also included in this figure is the maximum trim C_L obtained with the maximum horizontal-tail deflection of -6° .

Longitudinal control characteristics of the horizontal tail and the elevator for both Mach numbers are presented in figure 15 where the deflection angle required for trim is shown through the trim C_L range. Through the use of figure 14, the C_L required for level flight at several altitudes for a wing loading of 60 pounds per square foot was obtained for both Mach numbers and the values of i_t ($\delta_e = 0^\circ$) required for these conditions (from fig. 8(a)) are indicated in figure 15. It is shown that the stick-position stability (variation of i_t for trim with Mach number) for a constant wing loading is a function of altitude inasmuch as a stable condition (down deflection with increasing Mach number) exists at altitudes of 70,000 feet and 60,000 feet whereas an unstable condition is apparent at 40,000 feet. It should be pointed out, however, that the variation of wing loading with Mach number (weight decrease due to fuel consumption) is such that the stick-position stability would tend to increase.

The variation of trim C_L with horizontal-tail deflection (fig. 8(a)) was used to determine the incremental normal accelerations possible for various initial lifts. These results are shown in figure 16 for both Mach numbers.

The variation of several pertinent aerodynamic parameters through a Mach number range from 0.6 to 2 is presented in figure 17. Results in the subsonic range and at $M = 1.2$ were obtained from reference 2 while results from the present investigation were used to extend the variations to $M = 2$. Symbols on the curves of C_L and C_D for $\alpha = 0^\circ$ are actual test points and indicate the Mach numbers at which the experimental results were obtained. Those parameters obtained from slope measurements or derived from the measured data are shown as solid lines. Dashed lines shown in some cases indicate probable variations of the parameters with Mach number in those regions where no experimental results were obtained. Slope values were measured near $\alpha = 0^\circ$.

The change previously mentioned in stick-position stability with Mach number at supersonic speeds is shown in the variation of i_t for trim with Mach number ($\delta_e = 0^\circ$). At altitudes of 0, 20,000, and 40,000 feet for a wing loading of 65 pounds per square foot, the variation of i_t for trim with M indicates an upward deflection with increasing Mach number whereas at an altitude of 60,000 feet a downward deflection is required.

CONCLUSIONS

The results of the static longitudinal stability and control investigation at Mach numbers of 1.61 and 2.01 of a 1/16-scale model of the Douglas D-558-II research airplane indicated the following conclusions:

1. A high degree of longitudinal stability was obtained that decreased slightly with increasing Mach number and lift coefficient.
2. The maximum trim lift coefficient obtained with a maximum horizontal-tail deflection of -6° was 0.557 at $M = 1.61$ and 0.425 at $M = 2.01$.
3. The maximum trim L/D was 3.25 at $M = 1.61$ and 2.97 at $M = 2.01$.
4. For a constant wing loading the control deflection required for trim with increasing Mach number (stick-position stability) was found to change from an unstable to a stable variation with increasing altitude.

Langley Aeronautical Laboratory,
National Advisory Committee for Aeronautics,
Langley Field, Va., August 31, 1953.

REFERENCES

1. Grant, Frederick C., and Robinson, Ross B.: Static Lateral Stability Characteristics of a 1/16-Scale Model of the Douglas D-558-II Research Airplane at Mach Numbers of 1.61 and 2.01. NACA RM L53I29a, 1953.
2. Osborne, Robert S.: High Speed Wind-Tunnel Investigation of the Longitudinal Stability and Control Characteristics of a 1/16-Scale Model of the D-558-2 Research Airplane at High Subsonic Mach Numbers and at a Mach Number of 1.2. NACA RM L9C04, 1949.

TABLE I

DIMENSIONS OF THE 1/16-SCALE MODEL OF THE D-558-II

Wing:

Root airfoil section (normal to 0.30 chord)	NACA 63-010
Tip airfoil section (normal to 0.30 chord).	NACA 63-010
Total area (including fuselage intercept), sq ft	0.684
Span, in.	18.72
Mean aerodynamic chord, in.	5.46
Root chord (parallel to plane of symmetry), in.	6.78
Tip chord (parallel to plane of symmetry), in.	3.83
Taper ratio	0.565
Aspect ratio	3.57
Sweep of 0.30 chord line, deg	35
Incidence at fuselage center line, deg	3
Dihedral, deg	-3
Geometric twist, deg	0

Horizontal Tail:

Root airfoil section (normal to 0.30 chord)	NACA 63-010
Tip airfoil section (normal to 0.30 chord).	NACA 63-010
Area (including fuselage intercept), sq ft	0.156
Span, in.	8.98
Mean aerodynamic chord, in.	2.61
Root chord (parallel to plane of symmetry), in.	3.35
Tip chord (parallel to plane of symmetry), in.	1.68
Taper ratio	0.50
Aspect ratio	3.59
Sweep of 0.30 chord line, deg	40
Dihedral, deg	0
Elevator area, sq ft	0.059

Vertical Tail:

Airfoil section (parallel to fuselage center line) . . .	NACA 63-010
Area, sq ft	0.126
Span (from fuselage center line), in.	5.25
Root chord (parallel to fuselage center line), in.	9.14
Tip chord (parallel to fuselage center line), in.	2.75
Sweep of 0.30 chord, deg	49
Rudder area, sq ft	0.030

TABLE I.- Concluded.

DIMENSIONS OF THE 1/16-SCALE MODEL OF THE D-558-II

Fuselage:

Length, in.	31.50
Maximum diameter, in.	3.75
Fineness ratio	8.40
Base diameter, in.	1.56

TABLE II

COORDINATES OF THE BODY

[x is distance along model center line
from nose of model; r is the radius;
all dimensions in inches]

x	r
0	0
1.000	.382
2.000	.719
3.000	1.010
4.000	1.256
5.000	1.457
6.000	1.614
7.000	1.729
8.000	1.806
9.000	1.851
10.000	1.871
11.000	1.875
16.250	1.875
17.000	1.872
18.000	1.858
19.000	1.833
20.000	1.794
21.000	1.743
22.000	1.679
23.000	1.602
24.000	1.513
24.297	1.485
31.500	.780

TABLE III

COORDINATES OF WING FENCES AND AIRFOIL SECTION
IN THE PLANE OF THE FENCES

[x is distance from the leading edge along center line of airfoil section; y is distance perpendicular to center line (see fig. 3); all dimensions in inches]

Airfoil section		Fence	
x	y	x	y
0	0	-----	-----
.334	.128	0.334	0.128
.955	.207	.955	.585
1.672	.249	1.672	.746
2.259	.259	2.259	.766
3.073	.219	3.073	.687
4.155	.125	4.155	.125
5.59	0	-----	-----

Figure 1.- System of stability axes. Arrows indicate positive values.

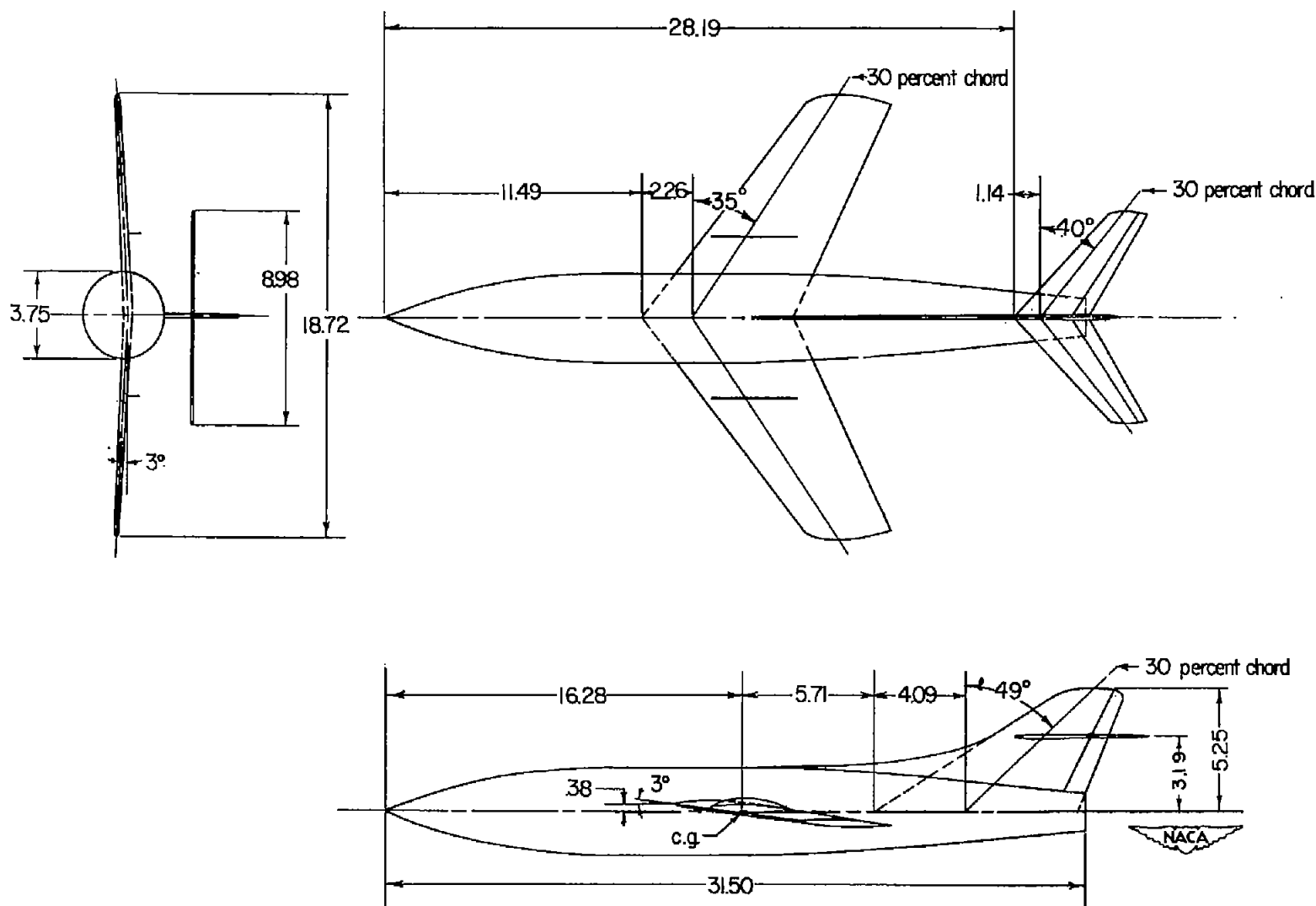


Figure 2.- Details of model. All dimensions in inches unless otherwise noted.

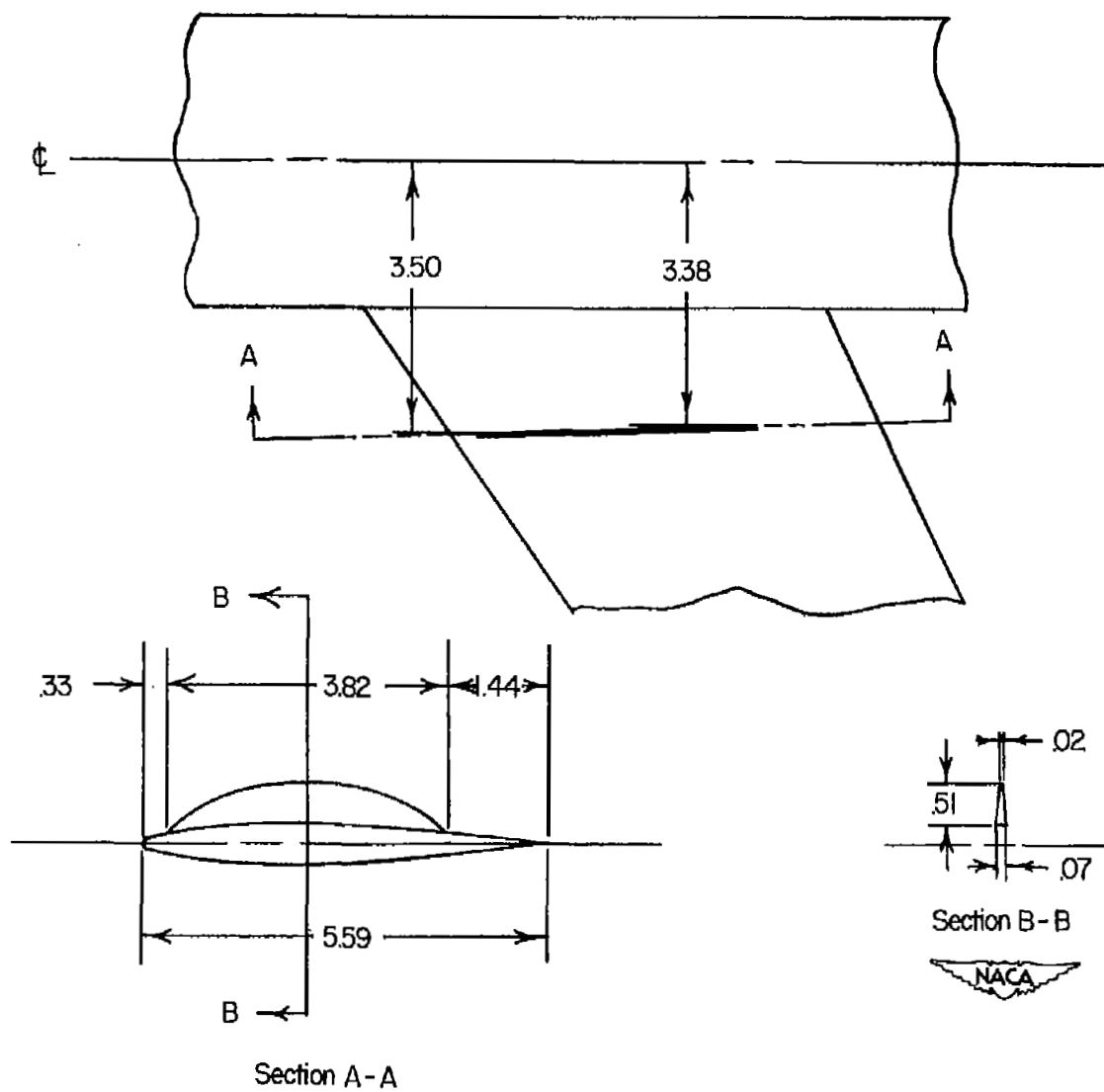


Figure 3.- Wing fence details. All dimensions in inches.

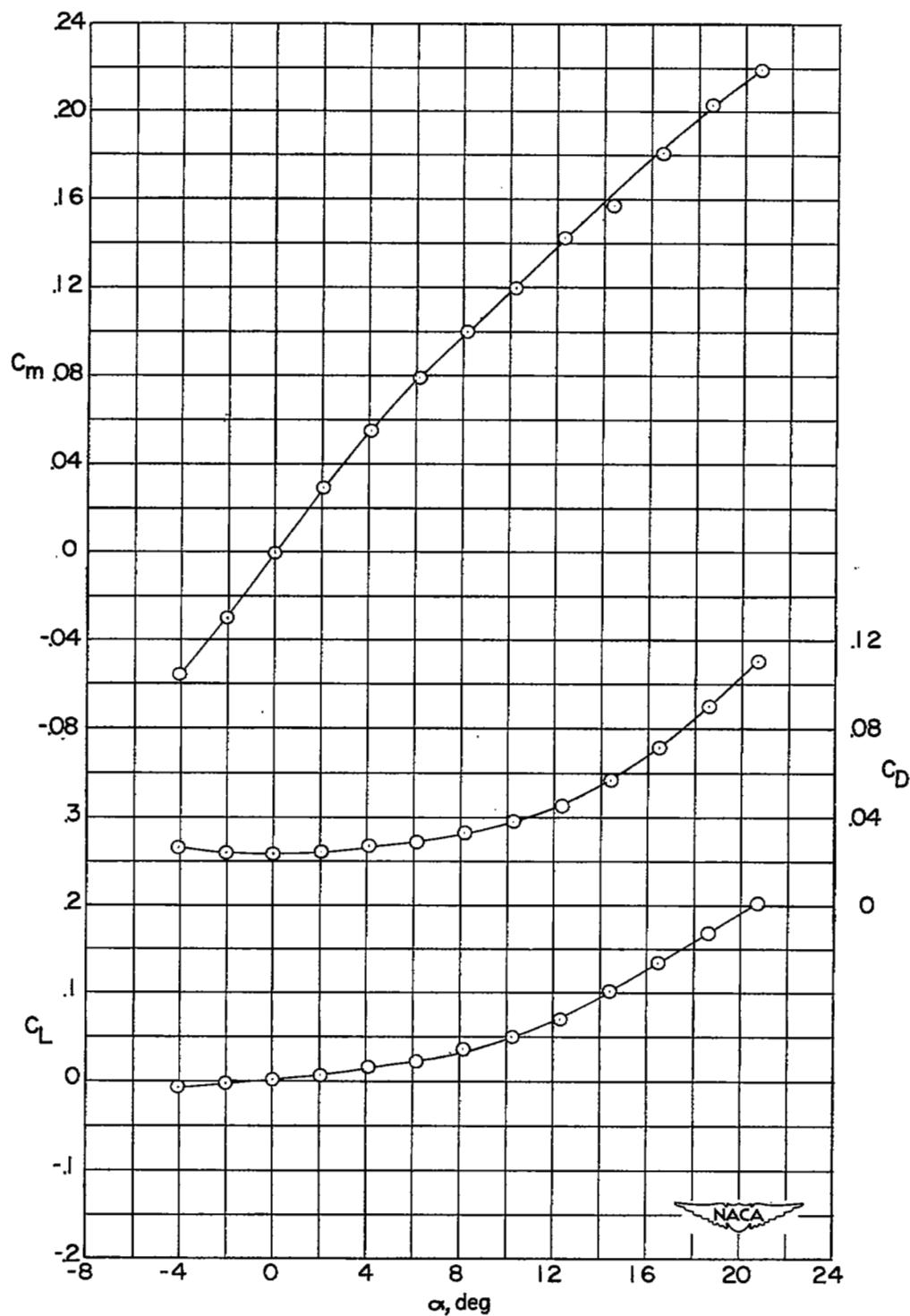
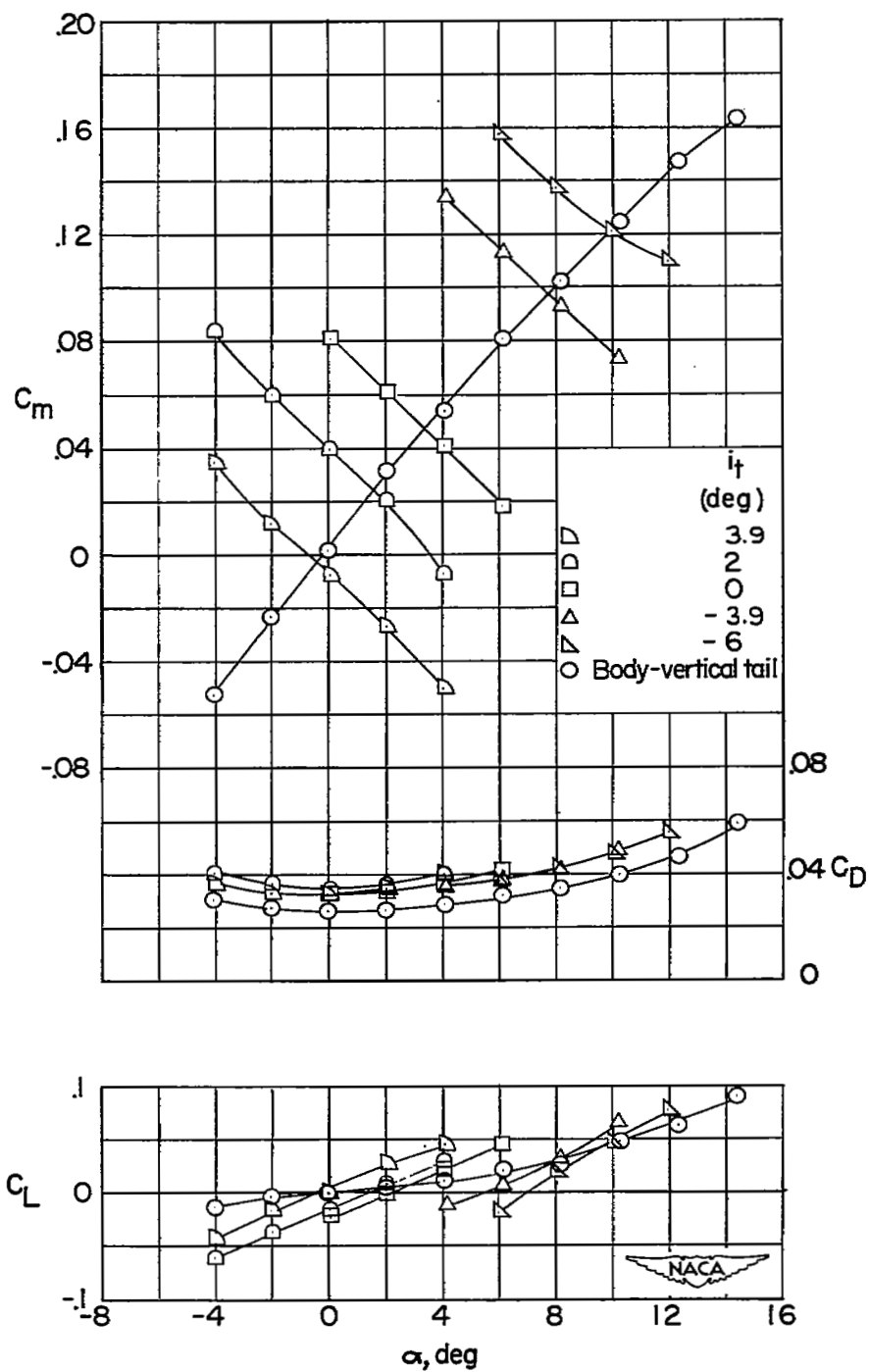


Figure 4.- Characteristics of body alone. $M = 1.61$.

(a) $M = 1.61$.Figure 5.- Characteristics of the body-tail configurations. $\delta_e = 0^\circ$.

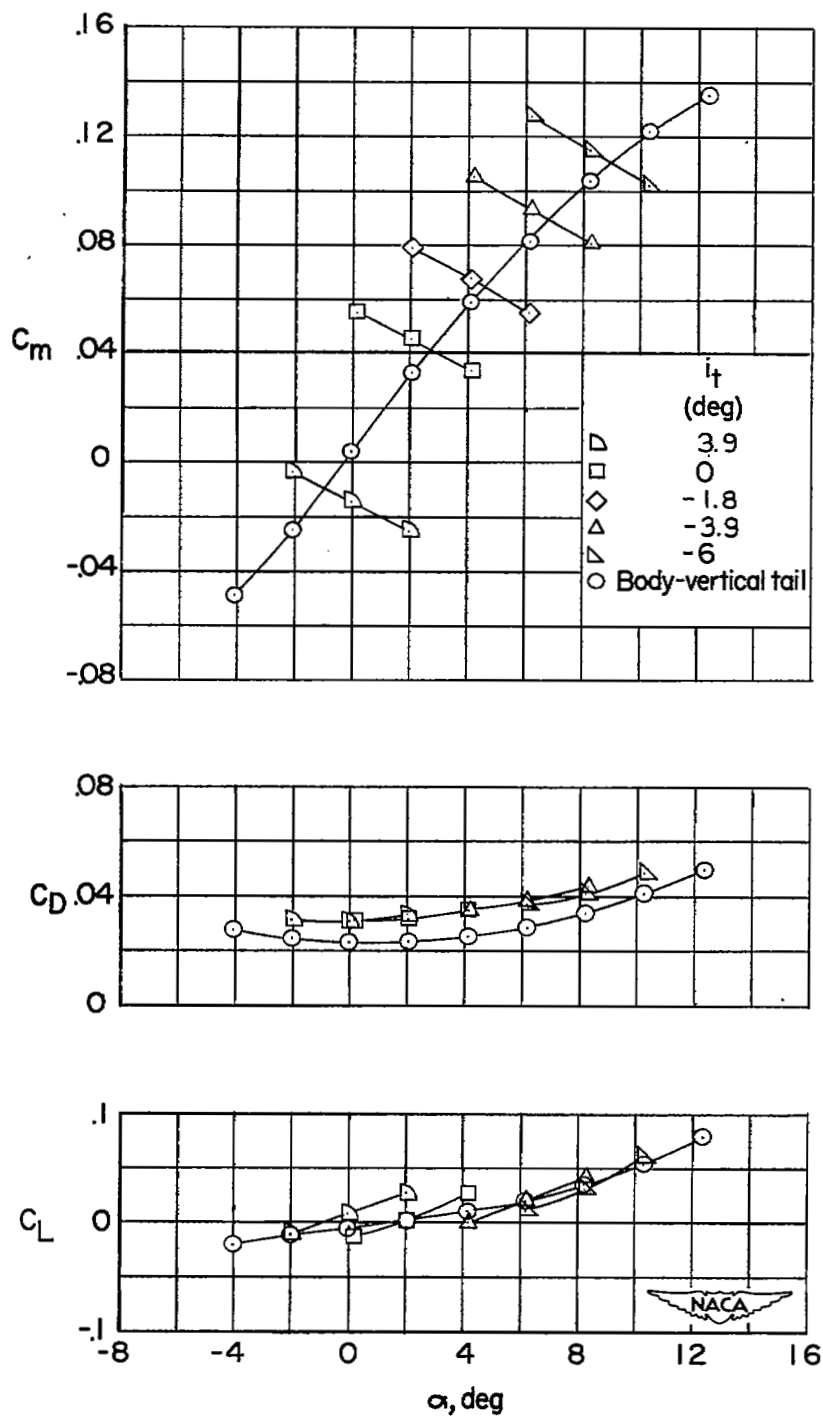
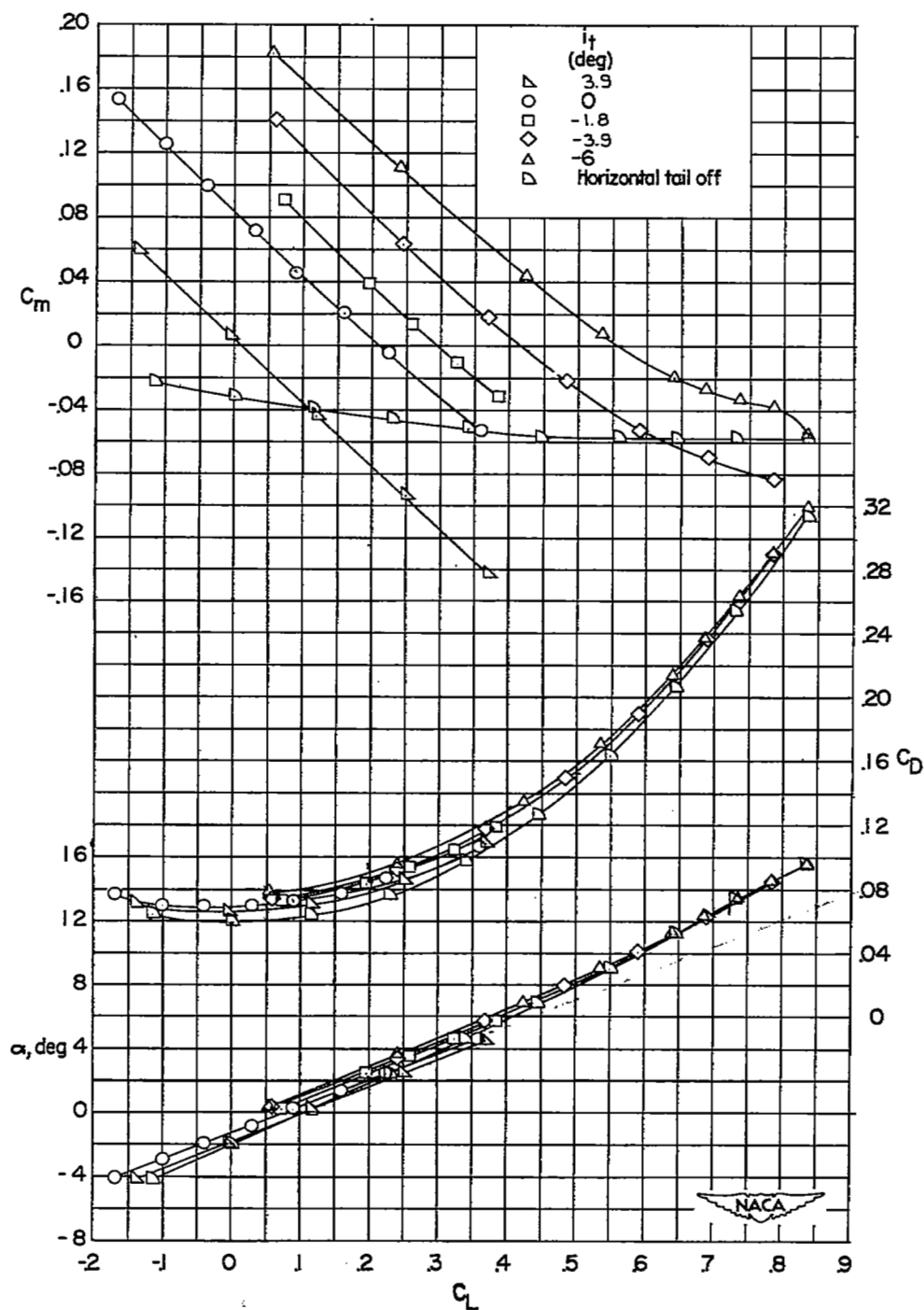
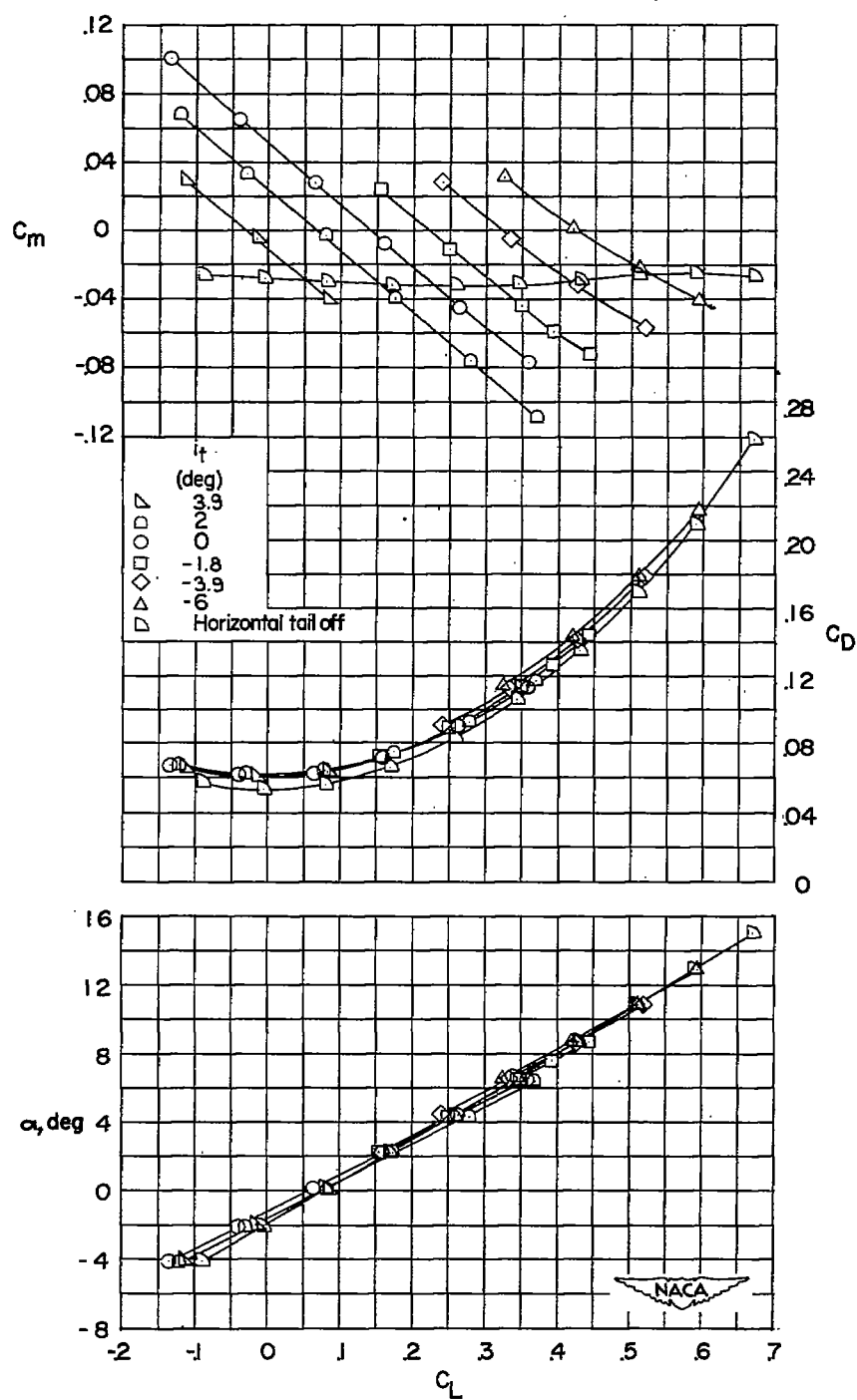
(b) $M = 2.01$

Figure 5.- Concluded.

(a) $M = 1.61$.Figure 6.- Characteristics of complete model with various horizontal tail angles. $\delta_e = 0$.



(b) $M = 2.01$.

Figure 6.- Concluded.

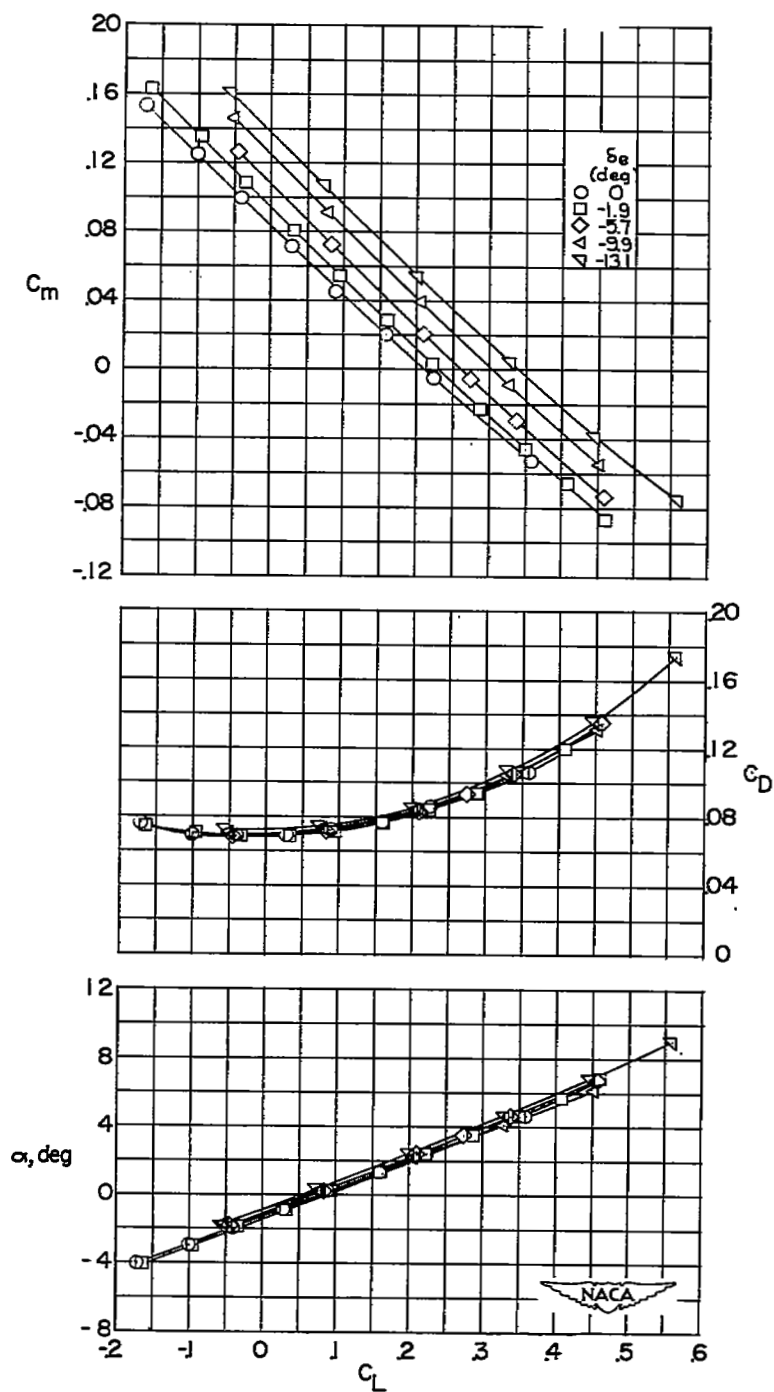
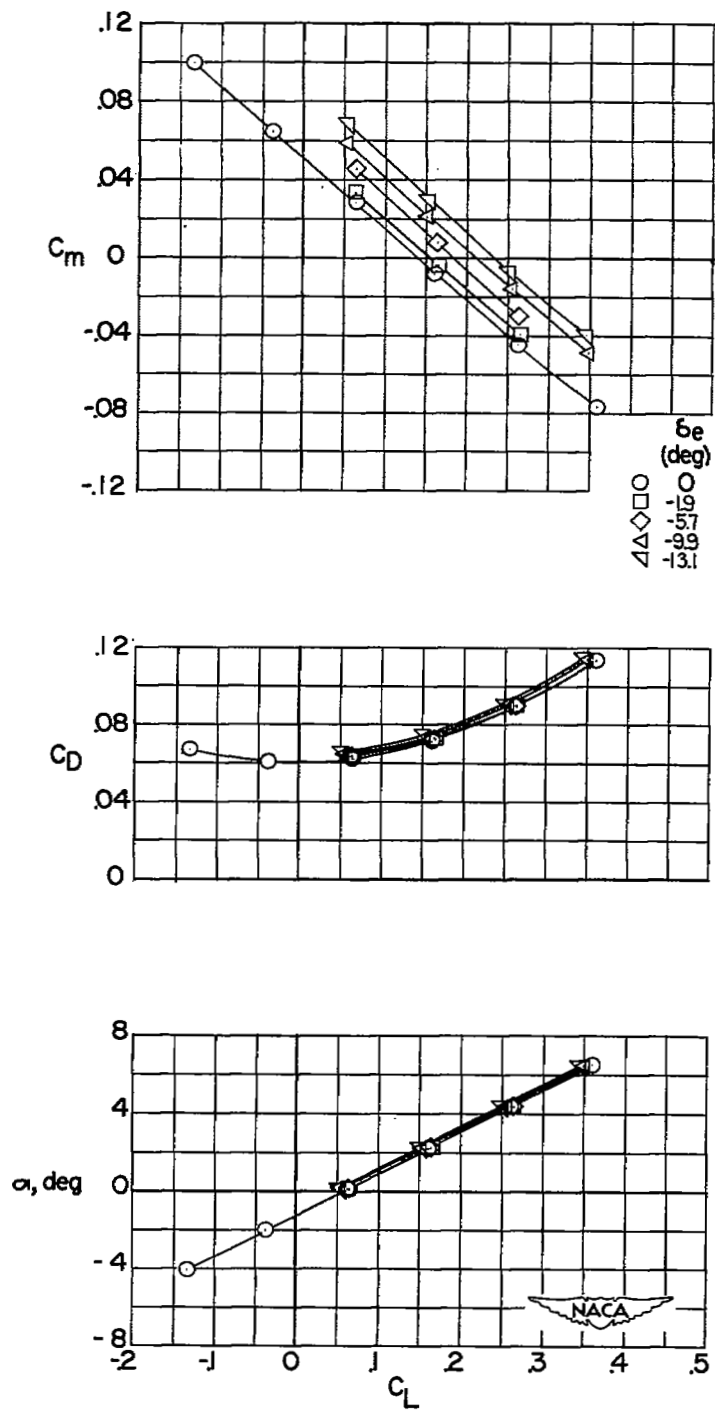
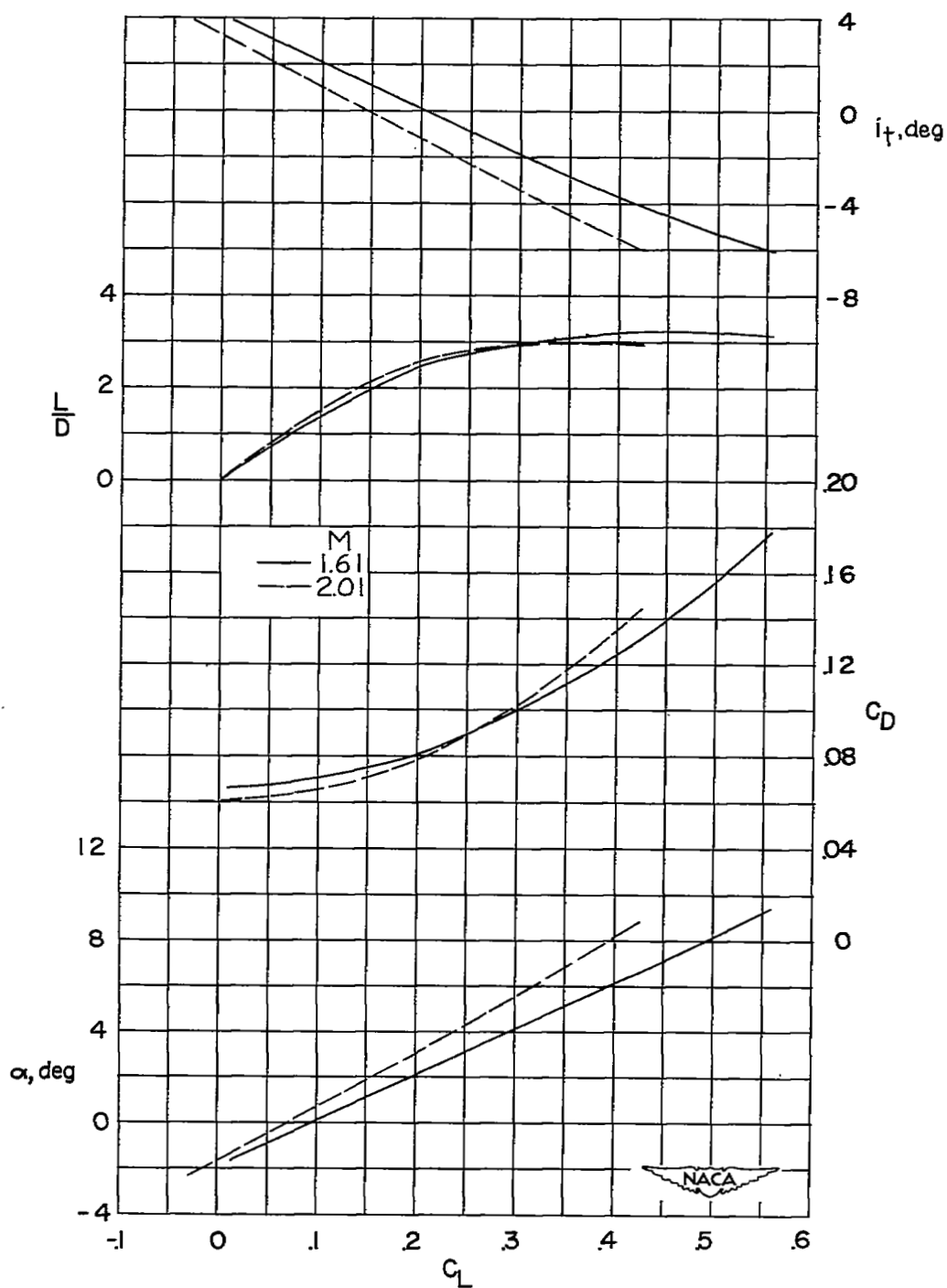
(a) $M = 1.61$.

Figure 7.- Effect of elevator deflection on complete model characteristics.
 $i_t = 0^\circ$.



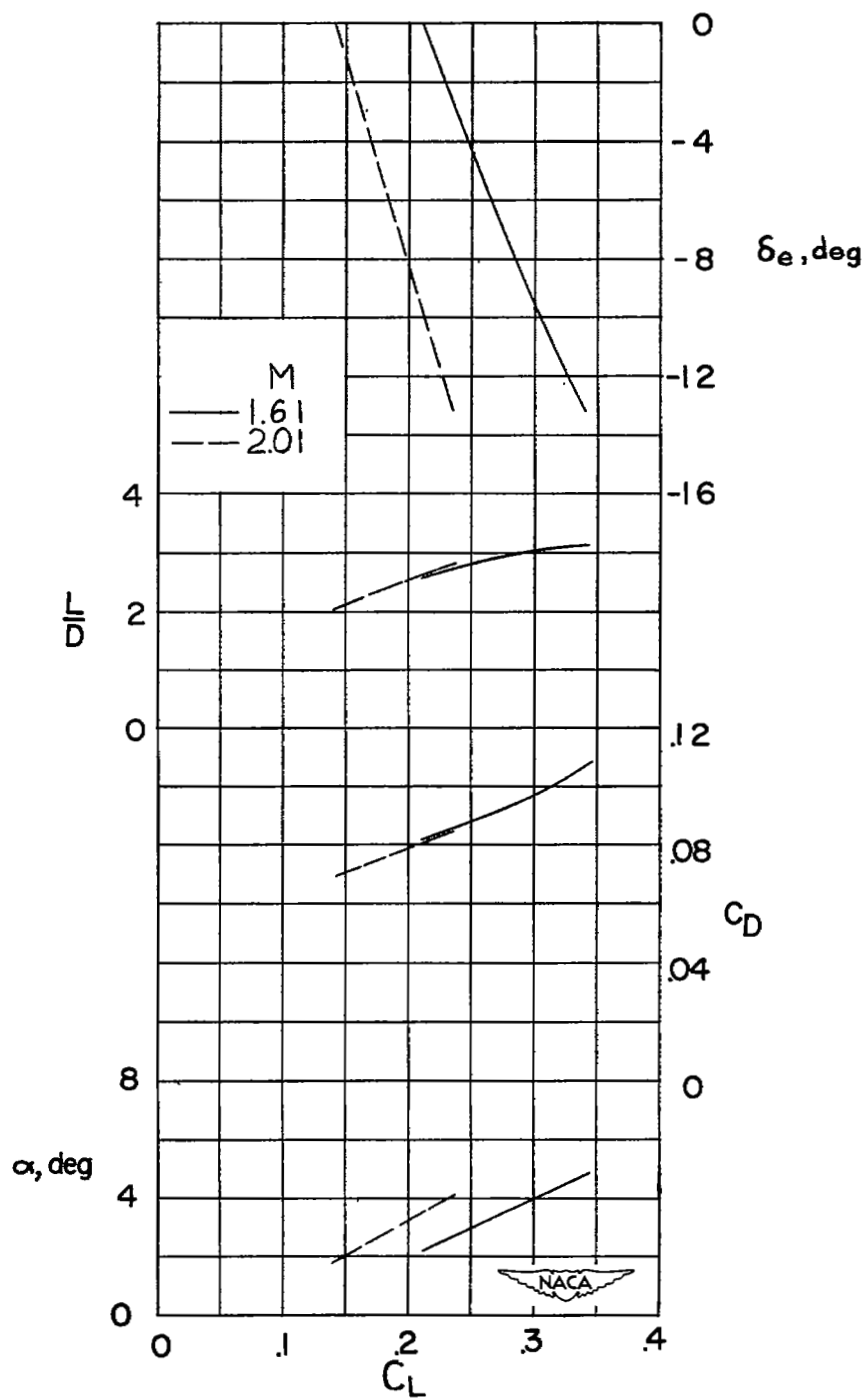
(b) $M = 2.01$.

Figure 7.- Concluded.



(a) Horizontal-tail control. $\delta_e = 0^\circ$.

Figure 8.- Longitudinal characteristics for trim. $C_m = 0$.



(b) Elevator control. $i_t = 0^\circ$.

Figure 8.- Concluded.

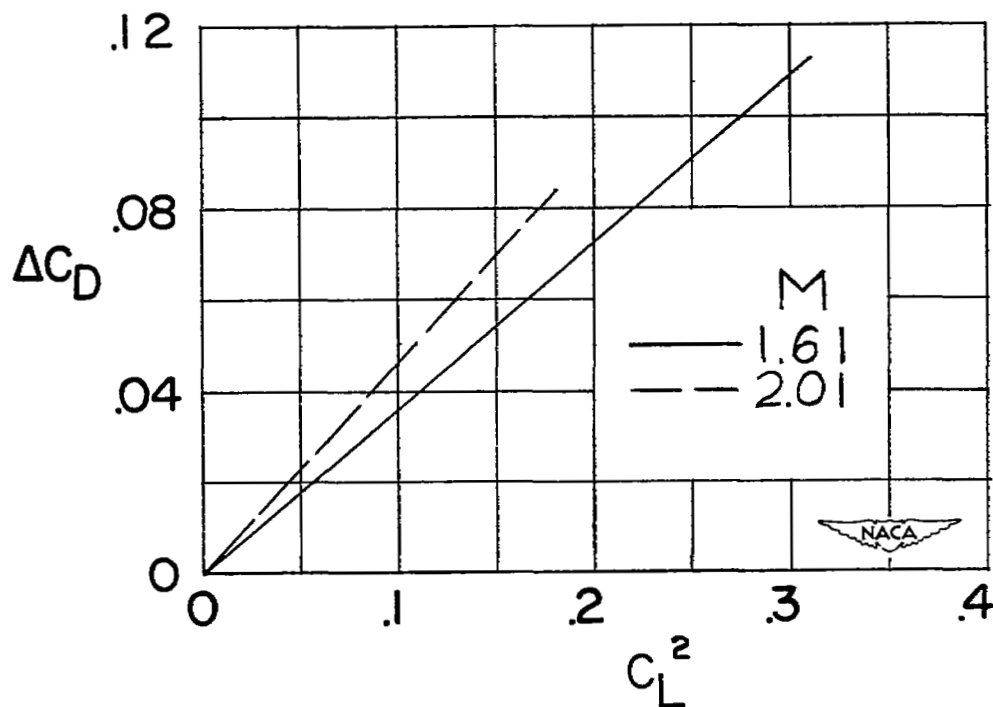


Figure 9.- Variation of drag with lift for trimmed flight.

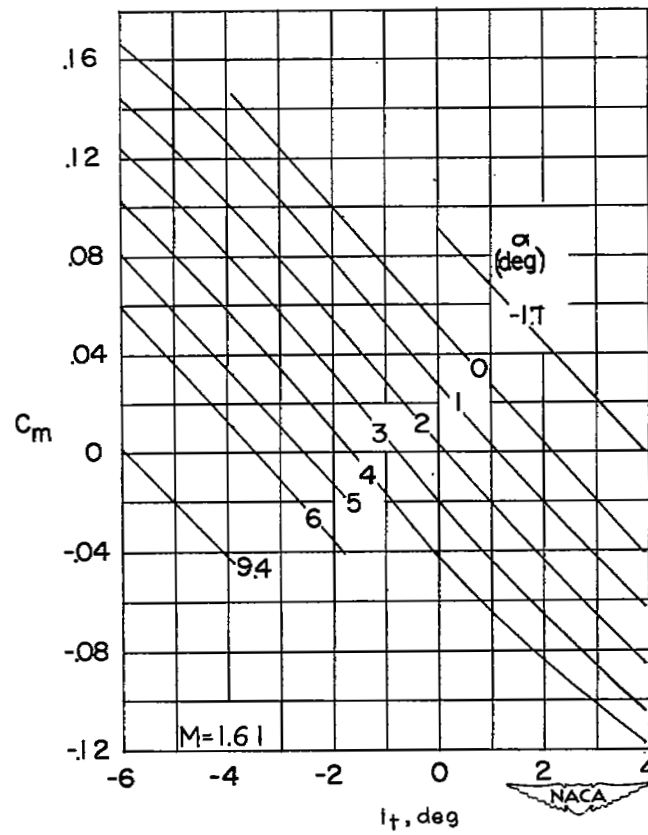
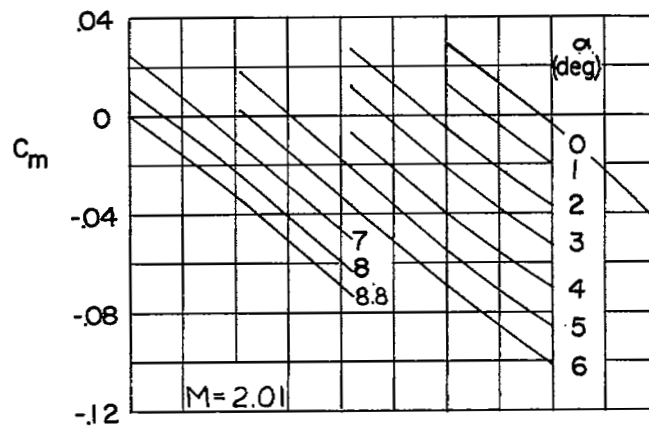


Figure 10.- Variation of pitching-moment coefficient with horizontal-tail deflection. $\delta_e = 0^\circ$.

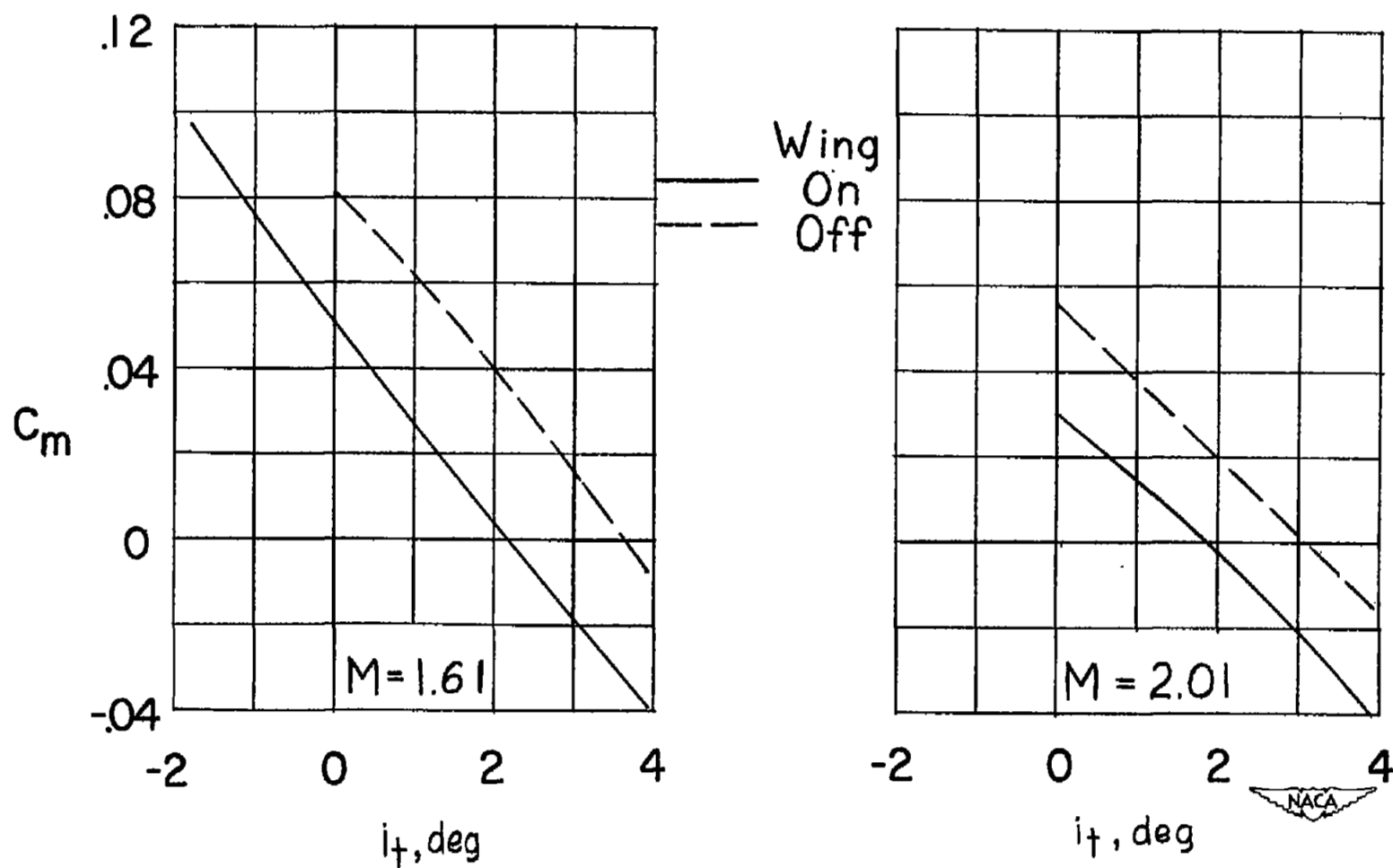


Figure 11.- Effect of wing on the variation of pitching-moment coefficient with horizontal-tail deflection. $\alpha = 0^\circ$; $\delta_e = 0^\circ$.

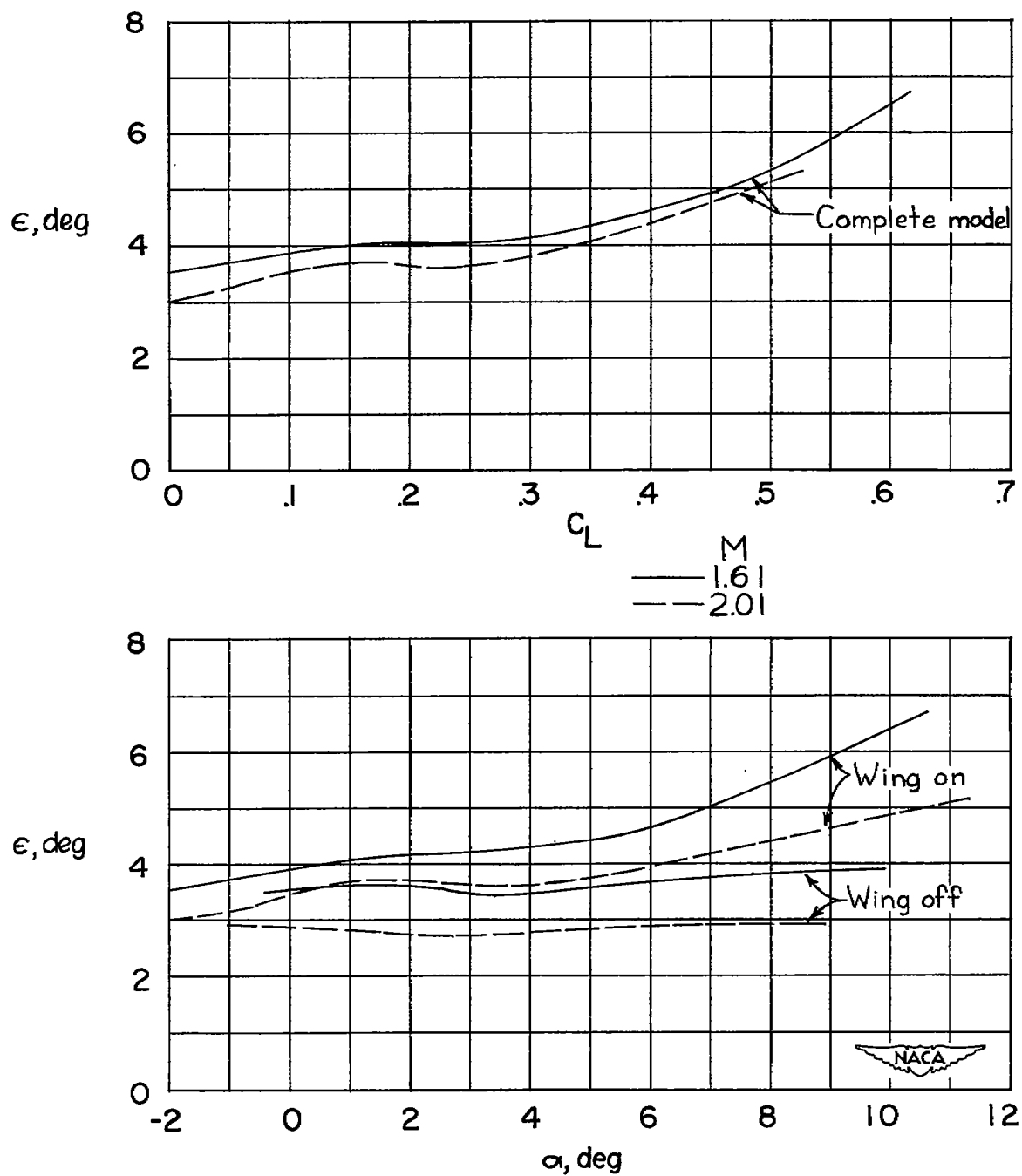


Figure 12.- Variation of effective downwash with lift coefficient and angle of attack.

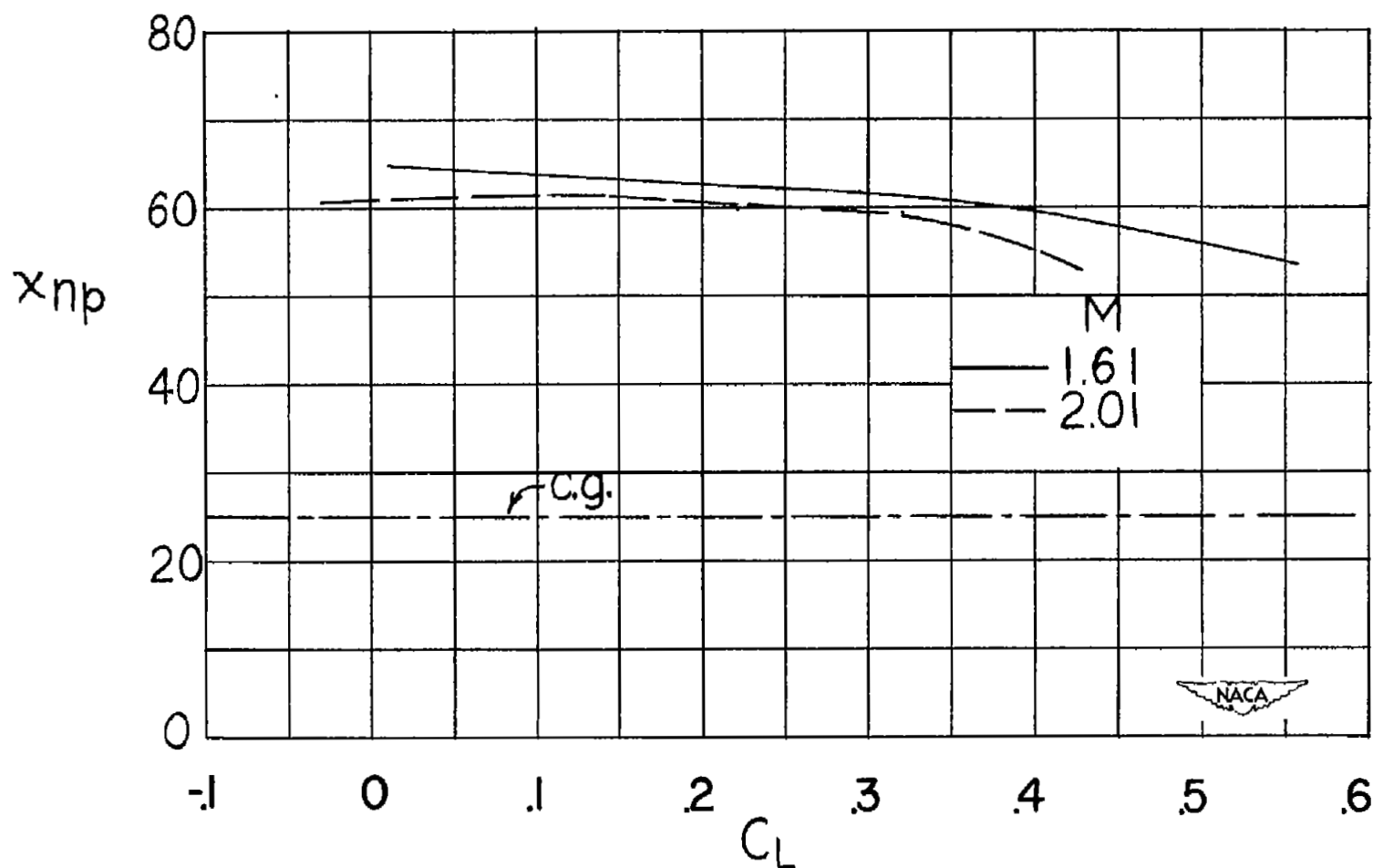


Figure 13.- Variation of neutral-point location with lift coefficient.

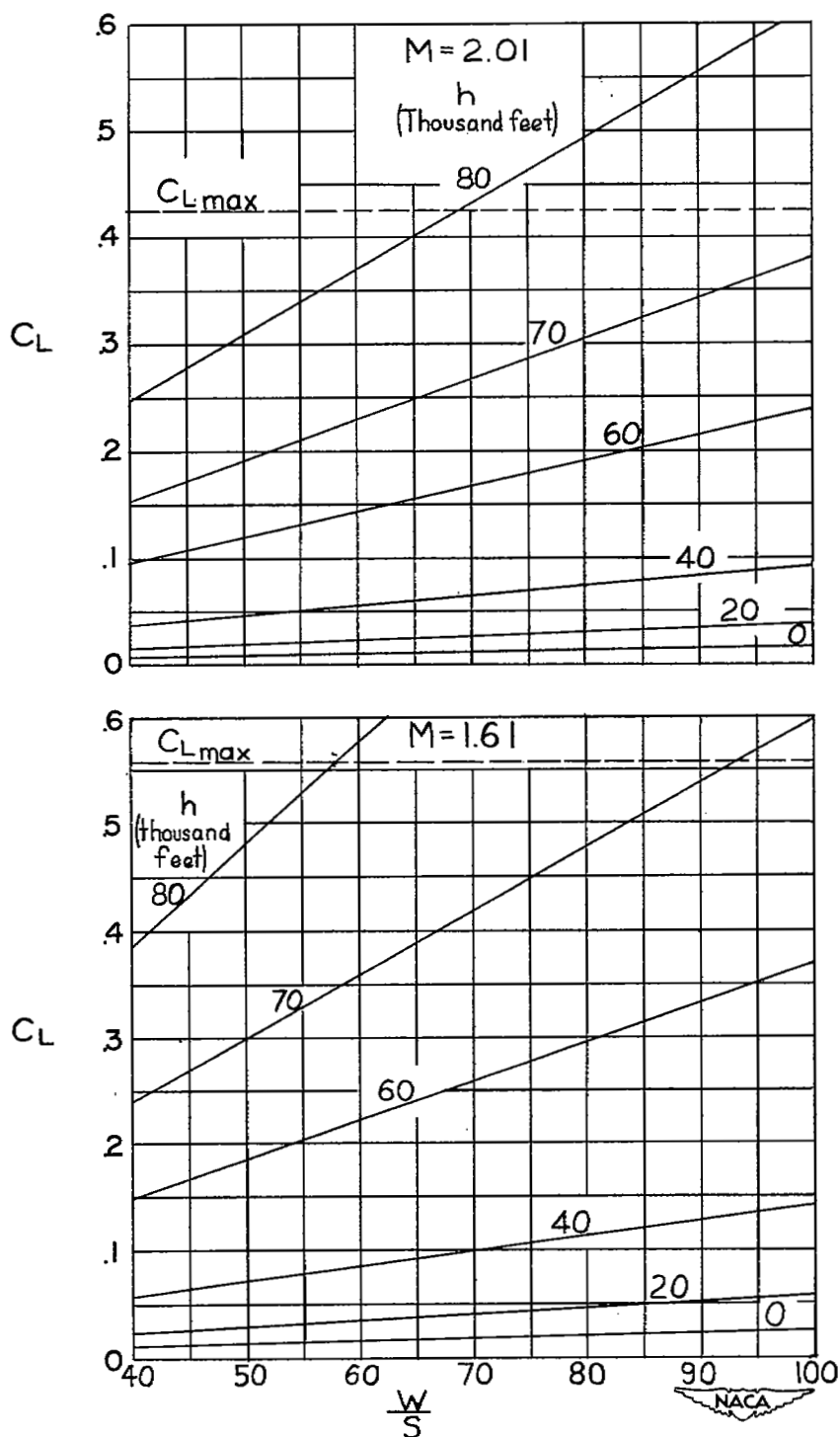


Figure 14.- Variation of lift coefficient required for level flight with altitude and wing loading.

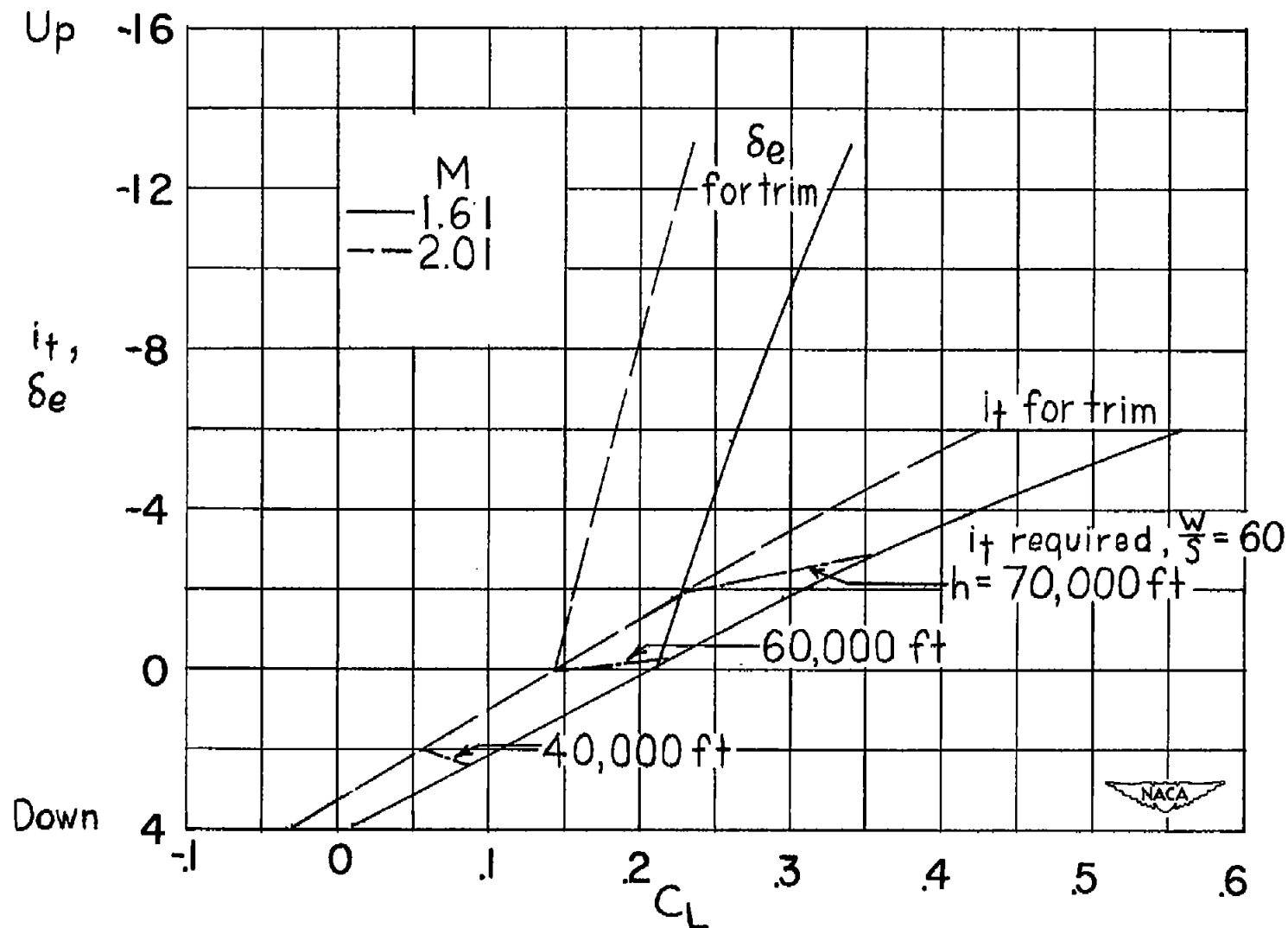


Figure 15.- Longitudinal control characteristics.

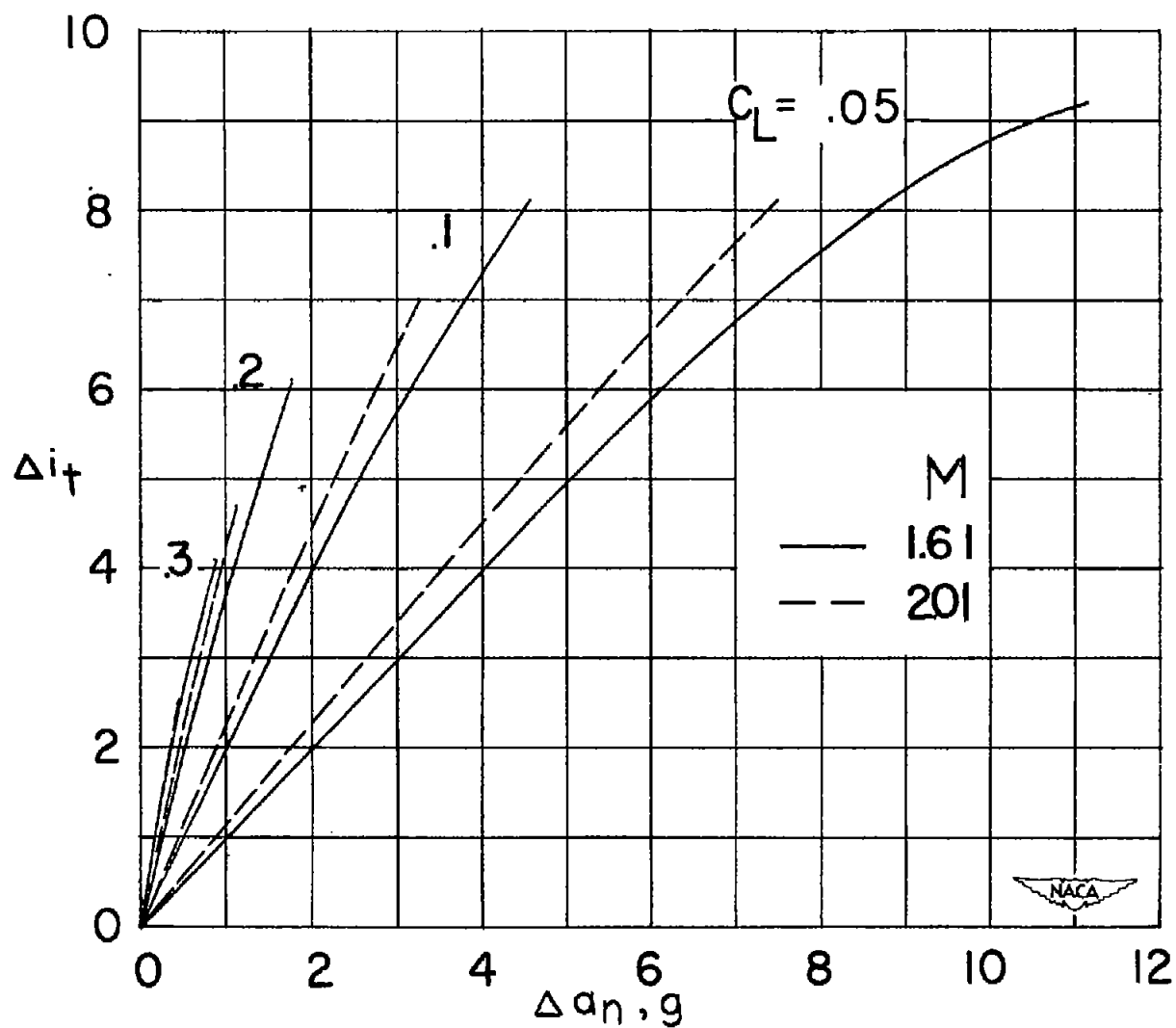


Figure 16.- Variation of normal acceleration with horizontal-tail deflection for several values of initial lift coefficient.

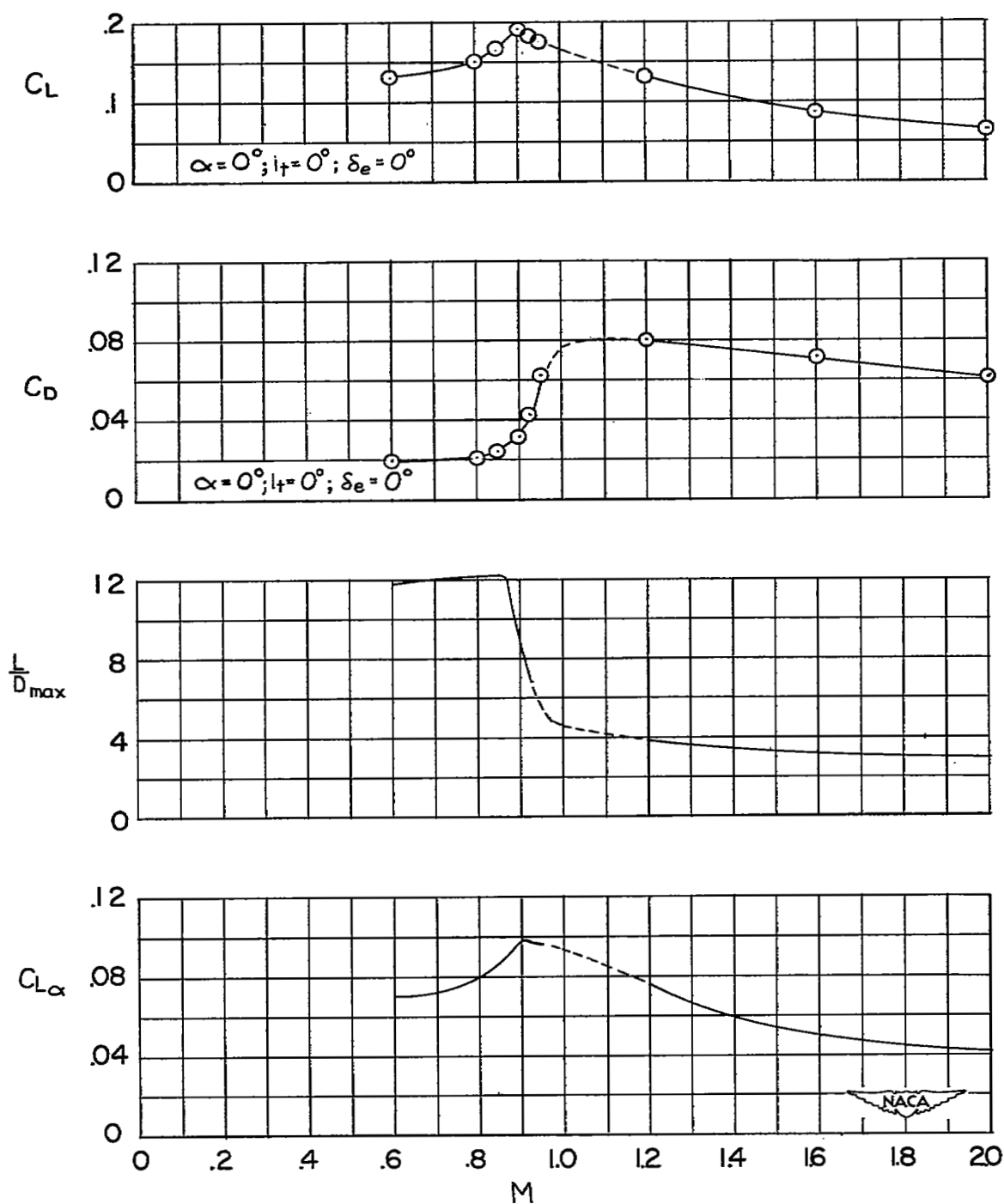


Figure 17.- Variation of various aerodynamic parameters with Mach number.

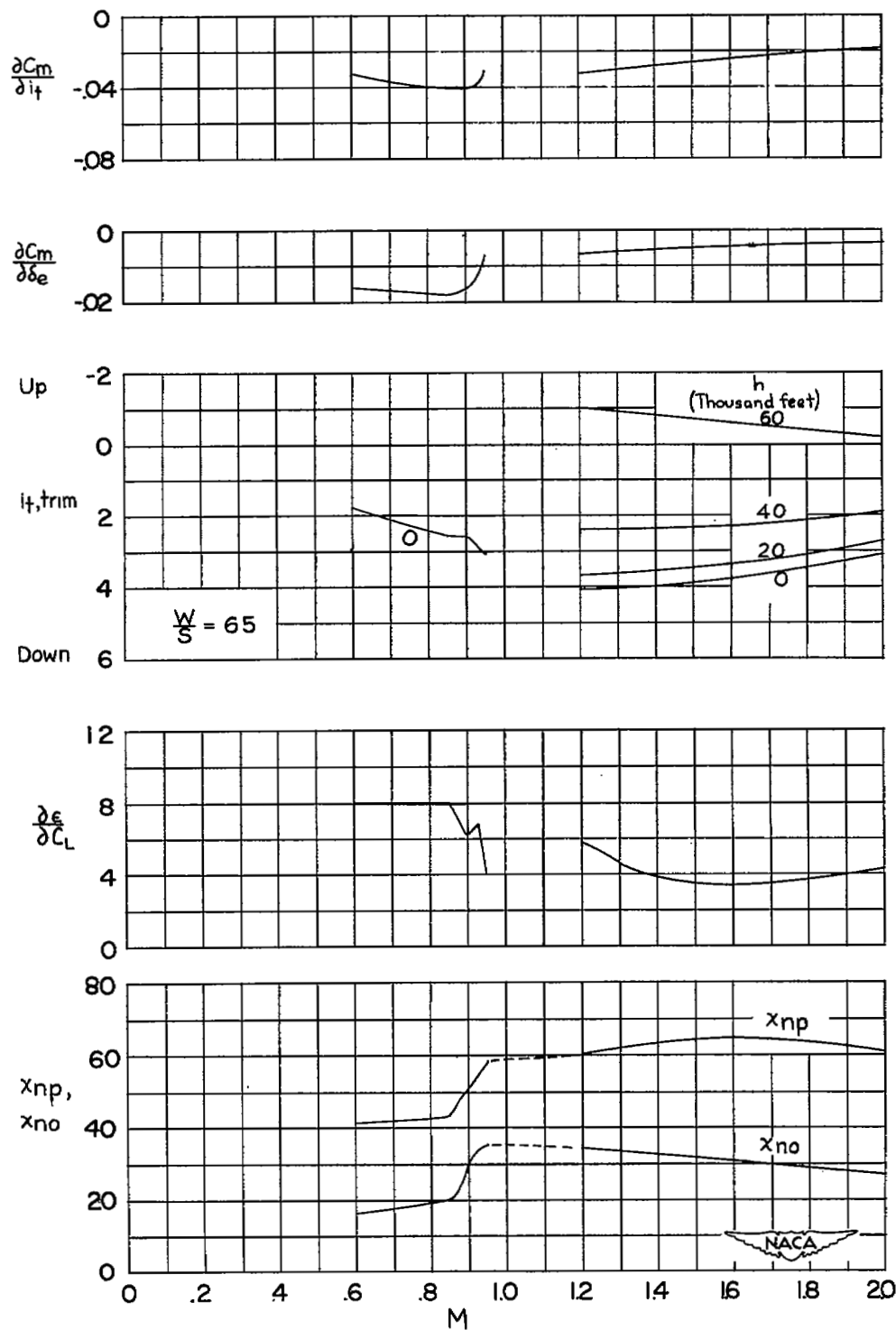


Figure 17.- Concluded.

~~SECURITY INFORMATION~~

NASA Technical Library



3 1176 01438 0217

~~CONFIDENTIAL~~